Progress In Electromagnetics Research C, Vol. 115, 95–110, 2021

Multiple Sources Localization Based on Independent Doublets Array

Jiacai Jiang*

Abstract—In this paper, an iterative algorithm for the location of multiple sources based on independent doublets arrays is proposed. The array brings a unified signal model for both near-field and far-field incoming sources. The signal model refrains the bias of Fresnel approximate due to the close displacement between elements of each doublet. Only exploiting the geometry of each doublet in direction-of-arrival (DOA) estimation, the proposed algorithm can avoid synchronization technology among different local oscillators of doublets, which means that elements among doublets could be independent. The proposed algorithm employs all the data received by the independent doublets arrays and can deal with more than two sources with only two coherent sensors in each doublet. The algorithm provides a simple approach and obtains acceptable results. Simulation results are illustrated to verify the effectiveness of the proposed algorithm.

1. INTRODUCTION

The source localization using a passive sensor array has been studied by researchers for its wide applications including radar, radio astronomy, sonar, geophysics, oceanography, seismology, and biomedical [1–4]. The problem of source location requires to estimate two types of parameters, direction of arrivals (DOA) and range of sources to the sensor array. The problem is further subdivided into two estimation problems under different assumptions as follows.

Compared with the aperture of the array, source-to-sensor distance is remarkably large. It means that the received wavefront emitted from sources is planar, and DOAs whose each source impinges on different sensors of array are approximately equal. In this situation, sources are recognized as far-field sources, and only DOAs of sources are required to estimate. Focusing on far-field sources, lots of algorithms have been proposed and summarized in [5], such as multiple signal classification (MUSIC) [6] and estimation parameters via rotational invariance techniques (ESPRIT) [7].

When the range of sources to the sensor array is not sufficiently large compared with the diameter of array, the wavefront of sources signal are spherical. Thus DOAs that each source impinges on different sensors of array are different. The assumption of far-field sources is not suitable. In this situation, sources are considered to locate at the near-field of an array. Both DOAs and range are required to estimate. Mostly, algorithms for near-field sources exploiting subspace of source involve one or more dimensions search [8–11]. In contrast to the subspace-based approaches, others employ the likelihood function [12, 13] or linear prediction (LP) [14]. Those algorithms for near-field sources are based on the Fresnel approximate model [15]. However, the model based on Fresnel approximation of near-field sources is modeling-mismatch and introduces a systematic error [15, 16]. The bias between the real model and Fresnel approximate model is non-random and adds towards random estimation errors with the additive noise.

In this paper, we focus on multiple sources localization by employing independent doublets arrays. The array is considered that each subarray involves two well calibrated elements, and elements between

Received 26 June 2021, Accepted 6 August 2021, Scheduled 6 September 2021

* Corresponding author: Jiacai Jiang (jiacaijiang@126.com).

The author is with the China Electronics Technology Group Corporation, No. 10 Research Institute, Chengdu 610036, Sichuan, China.

subarrays are independent for different oscillators. The received data model of the array can cope with a unified form for both far-field and near-field sources. Besides, the model can overcome the modeling-mismatch of near-field source.

The array appears like the array that bearing-only target location algorithms [17–20] employ. Actually, it is different from bearing-only location algorithms since those algorithms require two or more sensors in each subarray. Besides, bearing-only location algorithms are considered that bearings of sources are measured by each subarray, without taking the whole data received by array into consideration. Thus, those algorithms cannot obtain the optimal estimator. The proposed algorithm utilizes the whole data efficiently and can handle multiple sources with only two sensors in each doublet. Other location algorithms based on separated subarrays [21–23] also take all received data into consideration. These algorithms imply that all elements of array exploit a common oscillator or multiple well-synchronized oscillators. However, the array is hard to employ a common oscillator as the aperture of array becomes large. Besides, the synchronization technology for multiple oscillators costs too much and is difficult to apply. Since the proposed algorithm only utilizes the relationship between elements of each doublet, it can avoid the complex synchronization among oscillators of doublets and reduce the difficulty for application.

The proposed algorithm that we previously presented in [24] can only deal with the problem of location for single source. In this paper, we present an iterative algorithm to estimate parameters of multiple sources. The new algorithm exploits the iterative process to obtain angles that each source impinges on every doublet of array. Based on the estimated angles, the type of sources can be determined, and the range of near-field sources can be obtained by triangulation.

2. PROPOSED SIGNAL MODEL

Let us assume that there is a linear array composed of M doublets. As shown in Fig. 1, each doublet is composed of two elements. The displacement d of each doublet is measured in half-wavelength, and the displacement between m-th and $(m+1)$-th doublets is D_m, with $m = 1, 2, \ldots, M-1$.

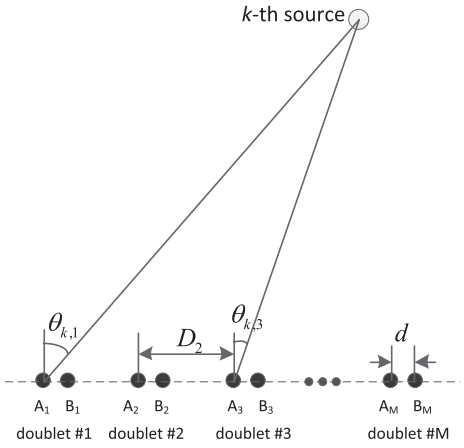

Figure 1. The subarray partition of the array.

The following assumptions are considered regarding the array, the signal sources, and the noise.

(i) The number of sources K is known, and it is smaller than the number of doublets M.

(ii) Sources are narrowband and independent of each other. Sources are located at the far-field of each doublet.

(iii) The sensor outputs are observed for a common time interval, which is longer than the random process correlation time and the time that sources wavefronts propagate across the array.

(iv) The amplitude gradient of the noisy signal across the array is negligible.

(v) The noise is considered independent, identically distributed Gaussian random variables with zero mean and σ^2 variance.

(vi) Elements in each doublet share a common local oscillator, and elements between doublets employ different local oscillators.

Sources are assumed to locate at the far-field of each doublet. It means that directions in which each source impinges on the two elements of each doublet are quite close, and the wavefront of signal source can be regarded as planar. Sources are also considered to locate at the near-field of the array; therefore, directions in which each source impinges on different doublets are quite different, and the wavefronts of signal source are regarded as circular. It is clear that sources located at the far-field of the array is a special case, and the sources are also located at the near-field of the array, where directions, whose each source impinges on different doublets, are the same. Suppose the kth source impinging upon the array from angle $\theta_{k,m}$ and range $r_{k,m}$ corresponding to the mth doublet. Thus, the aperture d of each doublet handles $r_{k,m} \gg 2d^2/\lambda$, with $m = 1, 2, \ldots, M$ and $k = 1, 2, \ldots, K$.

2.1. Signal Model

The phase shift associated with propagation time that the k-th source impinges on the element A_m of array is

$$\tau_{k,m} = 2\pi r_{k,m}/\lambda, \tag{1}$$

where λ is the wavelength of sources. Then, the received data of element A_m of the array are

$$\begin{aligned} x_{A_m}(t) &= \phi_m(t) \sum_{k=1}^{K} \exp(j\tau_{k,m}) s_k(t) + n_{A_m}(t) \\ &= \phi_m(t)\, \mathbf{c}_{A_m} \mathbf{s}(t) + n_{A_m}(t), \end{aligned} \tag{2}$$

where $\phi_m(t)$ is the phase of the m-th local oscillator of the m-th doublet, $s_k(t)$ the voltage at the terminals of the array element of the k-th source, $n_{A_m}(t)$ the received noise of array element A_m, and $\mathbf{c}_{A_m}$ is a $1 \times K$ steering vector, given by

$$\mathbf{c}_{A_m} = [\exp(j\tau_{1,m}), \exp(j\tau_{2,m}), \ldots, \exp(j\tau_{K,m})]. \tag{3}$$

The vector $\mathbf{s}(t) = [s_1(t), s_2(t), \ldots, s_K(t)]^T$ is the $K \times 1$ waveform vector. The symbol $(\cdot)^T$ represents the transposition.

Assume that the down-converter frequency of receivers equals the carrier frequency of sources, then the phase $\phi_m(t)$ is given by

$$\phi_m(t) = \exp[j\varphi_m(t) + j\varphi_{m,0}], \tag{4}$$

where $\varphi_m(t)$ is the phase noise of the m-th local oscillator of the m-th doublet, and $\varphi_{m,0}$ is the corresponding initial phase. Generally, the cost of synchronisation for time and frequency of different oscillators is less than that of phase. The synchronisation methods for time and frequency have been developed [25–27]. Typical global positioning system based (GPS-based) oscillators with 10 MHz [28–30] are with short-term stability of $\sigma_{Allan}(\Delta t = 1s) = 10^{-12}$ and short-term accuracy of 10^{-11}. Besides, the sample time of typical system for sources location is less than 1 ms. As a typical example, assuming 1 GHz center frequency location system, the phase produced by frequency bias varies slightly [31] and is less than 1°, which can be considered to be fast-time [32], and the phase noise of oscillator is negligible. Therefore, $\phi_m(t)$ can be approximated to a constant,

$$\phi_m(t) \approx \phi_m = \exp(j\varphi_{m,0}). \tag{5}$$

Thus, Equation (2) can be rewritten as

$$x_{A_m}(t) = \phi_m \mathbf{c}_{A_m} \mathbf{s}(t) + n_{A_m}(t). \tag{6}$$

Under the assumption that sources are located at the far-field of each doublet, the received data of element B_m of the array are

$$\begin{aligned} x_{B_m}(t) &= \phi_m \sum_{k=1}^{K} \upsilon_{k,m} \exp(j\tau_{k,m}) s_k(t) + n_{B_m}(t) \\ &= \phi_m (\boldsymbol{\upsilon}_m \odot \mathbf{c}_{A_m}) \mathbf{s}(t) + n_{B_m}(t), \end{aligned} \tag{7}$$

where $\upsilon_{k,m} = \exp(j\frac{2\pi d}{\lambda}\sin(\theta_{k,m}))$ is the phase difference for that the k-th source impinges on the elements A_m and B_m. $n_{B_m}(t)$ is the received noise of array element B_m. $\boldsymbol{\upsilon}_m$ is given by

$$\boldsymbol{\upsilon}_m = [\upsilon_{1,m}, \upsilon_{2,m}, \ldots, \upsilon_{K,m}], \tag{8}$$

the symbol $\odot$ denotes the Hadamard product.

The received data of subarray $\{A_1, A_2, \ldots, A_M\}$ are

$$\begin{aligned}\mathbf{x}_A(t) &= [x_{A_1}(t), x_{A_2}(t), \cdots, x_{A_M}(t)]^T \\ &= \left(\boldsymbol{\Phi}\bar{\mathbf{C}}_A\right)\mathbf{s}(t) + \mathbf{n}_A(t) \\ &= \mathbf{C_A}\mathbf{s}(t) + \mathbf{n}_A(t),\end{aligned} \tag{9}$$

where $\boldsymbol{\Phi} = \mathrm{diag}(\phi_1, \phi_2, \ldots, \phi_M)$. $\bar{\mathbf{C}}_A = \left[\mathbf{c}_{A_1}^T, \mathbf{c}_{A_2}^T, \cdots, \mathbf{c}_{A_M}^T\right]^T$. $\mathbf{C_A} \triangleq \boldsymbol{\Phi}\bar{\mathbf{C}}_A$.

The received data of subarray $\{B_1, B_2, \ldots, B_M\}$ are

$$\begin{aligned}\mathbf{x}_B(t) &= [x_{B_1}(t), x_{B_2}(t), \cdots, x_{B_M}(t)]^T \\ &= \left[\boldsymbol{\Phi}\left(\boldsymbol{\Upsilon} \odot \bar{\mathbf{C}}_A\right)\right]\mathbf{s}(t) + \mathbf{n}_B(t) \\ &= \mathbf{C}_B\mathbf{s}(t) + \mathbf{n}_B(t),\end{aligned} \tag{10}$$

where $\boldsymbol{\Upsilon}$ representing the phase shift matrix is given by

$$\boldsymbol{\Upsilon} = \left[\ \boldsymbol{\upsilon}_1^T, \boldsymbol{\upsilon}_2^T, \cdots, \boldsymbol{\upsilon}_M^T\ \right]^T. \tag{11}$$

$\mathbf{C}_B$ is the matrix defined by $\mathbf{C}_B \triangleq \boldsymbol{\Phi}\left(\boldsymbol{\Upsilon} \odot \bar{\mathbf{C}}_A\right)$.

The entire data received by the array are

$$\begin{aligned}\mathbf{x}(t) &= \left[\ \mathbf{x}_A^T(t) \quad \mathbf{x}_B^T(t)\ \right]^T \\ &= \begin{bmatrix}\mathbf{C}_A \\ \mathbf{C}_B\end{bmatrix}\mathbf{s}(t) + \begin{bmatrix}\mathbf{n}_A(t) \\ \mathbf{n}_B(t)\end{bmatrix}.\end{aligned} \tag{12}$$

Theorem 1 *[33] Let $\mathcal{D} \in \mathbb{C}^{M\times M}$ be diagonal matrix, and matrix $\mathcal{A} \in \mathbb{C}^{M\times N}$ and $\mathcal{B} \in \mathbb{C}^{M\times N}$, then*

$$\mathcal{D}(\mathcal{A} \odot \mathcal{B}) = (\mathcal{D}\mathcal{A}) \odot \mathcal{B} = \mathcal{A} \odot (\mathcal{D}\mathcal{B}).$$

With *Theorem 1*, the relationship between matrices $\mathbf{C}_A$ and $\mathbf{C}_B$ can be given by

$$\begin{aligned}\mathbf{C}_B &= \boldsymbol{\Phi}\left(\boldsymbol{\Upsilon} \odot \bar{\mathbf{C}}_A\right) \\ &= \mathbf{C}_A \odot \boldsymbol{\Upsilon} = \boldsymbol{\Upsilon} \odot \mathbf{C}_A.\end{aligned} \tag{13}$$

3. PROPOSED ALGORITHM

A maximum-likelihood (ML) estimator is derived in Appendix A. However, the ML solution is computationally prohibitive in most practical applications. In this section, the optimization model for the signal model and corresponding iterative estimation is presented.

3.1. Generalized ESPRIT and Optimization Model

The covariance matrix of $\mathbf{x}(t)$ is

$$\begin{aligned}\mathbf{R} &= E[\mathbf{x}(t)\,\mathbf{x}^H(t)] \\ &= \begin{bmatrix}\mathbf{C}_A \\ \mathbf{C}_B\end{bmatrix}\mathbf{R}_s\begin{bmatrix}\mathbf{C}_A \\ \mathbf{C}_B\end{bmatrix}^H + \sigma^2\mathbf{I},\end{aligned} \tag{14}$$

where $\mathbf{R}_s = E\left[\mathbf{s}(t)\mathbf{s}^H(t)\right]$ denotes the diagonal matrix of sources power; σ^2 is the variance of noise; the symbol $(\cdot)^H$ denotes the conjugate transpose of matrix.

By eigen-decomposition of the covariance matrix $\mathbf{R}$, it is obtained that

$$\mathbf{R} = \mathbf{U}\boldsymbol{\Sigma}\mathbf{U}^H = \mathbf{U}_s\boldsymbol{\Sigma}_s\mathbf{U}_s^H + \mathbf{U}_n\boldsymbol{\Sigma}_n\mathbf{U}_n^H, \tag{15}$$

where $\mathbf{U_s}$ and $\mathbf{U_n}$ are the signal subspace and noise subspace, respectively.

Since the column space $\mathbb{R}\{\mathbf{U}_s\}$ of $\mathbf{U}_s$ equals the column space $\mathbb{R}\left\{\begin{bmatrix}\mathbf{C}_A\\ \mathbf{C}_B\end{bmatrix}\right\}$, there must exist a non-singular matrix $\mathbf{F}$, satisfying

$$\begin{bmatrix}\mathbf{C}_A\\ \mathbf{C}_B\end{bmatrix} = \mathbf{U}_s\mathbf{F} = \begin{bmatrix}\mathbf{U}_{s1}\\ \mathbf{U}_{s2}\end{bmatrix}\mathbf{F}, \tag{16}$$

where $\mathbf{U}_{s1}$ and $\mathbf{U}_{s2}$ are the two $M \times K$ submatrices of $\mathbf{U}_s$.

Therefore, it can be obtained that

$$\begin{aligned}\mathbf{U}_{s1} &= \mathbf{C}_A\mathbf{F}^{-1}\\ \mathbf{U}_{s2} &= \mathbf{C}_B\mathbf{F}^{-1} = (\boldsymbol{\Upsilon} \odot \mathbf{C}_A)\,\mathbf{F}^{-1}.\end{aligned} \tag{17}$$

where the superscript $(\cdot)^{-1}$ denotes the inverse.

It can be obtained that

$$\mathbf{U}_{s2} = [\boldsymbol{\Upsilon} \odot (\mathbf{U}_{s1}\mathbf{F})]\,\mathbf{F}^{-1}, \tag{18}$$

Equation (18) shows the inner relationship between the signal subspaces and steering matrices of array.

The matrix $\boldsymbol{\Upsilon}$ involving in all angles can be obtained by solving the following minimization problem:

$$\begin{aligned}&\min_{\boldsymbol{\Upsilon},\mathbf{F}} \left\|\mathbf{U}_{s2} - [\boldsymbol{\Upsilon} \odot (\mathbf{U}_{s1}\mathbf{F})]\,\mathbf{F}^{-1}\right\|_F,\\ &s.t. \quad \begin{cases} rank\,(\mathbf{F}) = K\\ rank\,(\boldsymbol{\Upsilon}) = K\\ |\upsilon_{m,k}| = 1\end{cases}.\end{aligned} \tag{19}$$

where $\|\cdot\|_F$ is the Frobenius matrix norm, and $\upsilon_{m,k}$ is the m-th row and k-th column element of matrix $\boldsymbol{\Upsilon}$. $m = 1, 2, \ldots, M$. $k = 1, 2, \ldots, K$.

3.2. Solution Method

3.2.1. Alternating Iterative Technique

It is clear that Equation (19) is a noncovex multi-dimensional optimization problem. Its globally optimal solutions can be gained with huge computational load. In this section, we propose an alternating iterative technique to reduce the computation.

By dropping all the rank constraints from Equation (19), the optimization problem can be relaxed into the following equation

$$\begin{aligned}&\min_{\boldsymbol{\Upsilon},\mathbf{F}} \left\|\mathbf{U}_{s2} - [\boldsymbol{\Upsilon} \odot (\mathbf{U}_{s1}\mathbf{F})]\,\mathbf{F}^{-1}\right\|_F,\\ &s.t. \quad |\upsilon_{m,k}| = 1.\end{aligned} \tag{20}$$

In order to simplify the problem, it is suggested to denote the first $\mathbf{F}$ and second $\mathbf{F}$ of Equation (20) as two independent matrices $\mathbf{F}_B$ and $\mathbf{F}_A$, respectively. It follows that the conditional least squares update of $\hat{\mathbf{F}}_A$ is given by

$$\hat{\mathbf{F}}_A = \mathbf{U}_{s2}^{\dagger}\left[\left(\mathbf{U}_{s1}\hat{\mathbf{F}}_B\right) \odot \hat{\boldsymbol{\Upsilon}}\right]. \tag{21}$$

where $(.)^{\dagger}$ denotes the pseudo-inverse of matrix.

The matrix $\hat{\boldsymbol{\Upsilon}}$ is estimated by

$$\hat{\boldsymbol{\Upsilon}} = \left(\mathbf{U}_{s2}\hat{\mathbf{F}}_A\right)./\left(\mathbf{U}_{s1}\hat{\mathbf{F}}_B\right). \tag{22}$$

where $(./)$ denotes the division of each element of two matrices. Finally, matrix $\hat{\mathbf{F}}_B$ can be replaced by the previous estimated $\hat{\mathbf{F}}_A$.

Alternating iterative technique can be initialized by the ESPRIT algorithm under reasonable assumption below. Note that the given initialized matrix $\hat{\mathbf{F}}_B$ may improve or maintain performance, without significant deterioration. From this observation, the solution will convergence to (at least) a local minimum following directly. The reasonable initial estimation can ensure that the global minimum is reached, and the optimal solution is guaranteed.

3.2.2. Initial Estimation

Obviously, when the range between sources and array is considered to be infinite, solutions of the problem are easy to obtain. The relevant matrices $\boldsymbol{\Upsilon}$ and $\mathbf{F}$ can be used as the initial value of the alternating iterative method. In this section, the initial estimation method for matrices $\boldsymbol{\Upsilon}$ and $\mathbf{F}$ is considered.

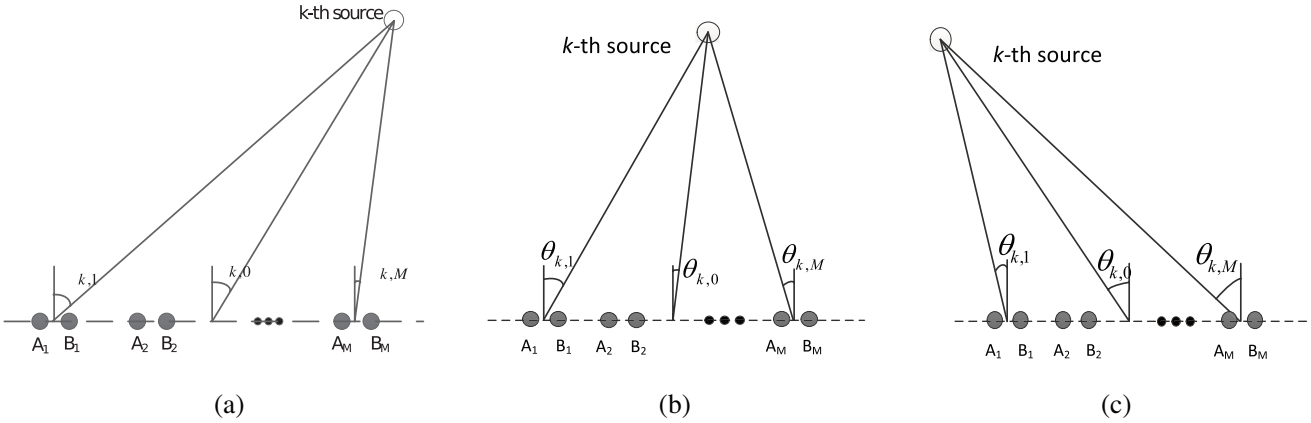

Figure 2. (a) The source is located in the right region of the array. (b) The source is located in the direct region of the array. (c) The source is located in the left region of the array.

The different relative relationships of direction between doublets and the sources are shown in Fig. 2. It is clear that $\theta_{k,1}, \theta_{k,2}, \ldots, \theta_{k,M}$ satisfy

$$\{\theta_{k,1}, \theta_{k,2}, \ldots, \theta_{k,M}\} \in [\theta_{k,1}, \theta_{k,M}], when, \theta_{k,1} \leqslant \theta_{k,M}, \tag{23}$$

or

$$\{\theta_{k,1}, \theta_{k,2}, \ldots, \theta_{k,M}\} \in [\theta_{k,M}, \theta_{k,1}], when, \theta_{k,M} \leqslant \theta_{k,1}. \tag{24}$$

To obtain the initial estimation of parameter, approximate processing is required. The range of sources is assumed to be large enough so that each source can be reasonably considered as a far-field source. Thus the angles $\theta_{k,1}, \theta_{k,2}, \ldots, \theta_{k,M}$ of the k-th source can be properly replaced with a common angle $\theta_{k,0}$ as shown in Fig. 2, where $\theta_{k,0}$ is a virtual angle. Then the corresponding phase difference is represented by a common value $\upsilon_{k,0}$, $\upsilon_{k,0} = \exp[j\frac{2\pi d}{\lambda}\sin(\theta_{k,0})]$. Apparently, the common angle $\theta_{k,0}$ for each far-field source is the actual angle of it. Therefore, the approximation of Equation (11) is

$$\boldsymbol{\Upsilon}_0 \approx \begin{bmatrix} \upsilon_{1,0} & \upsilon_{2,0} & \cdots & \upsilon_{K,0} \\ \upsilon_{1,0} & \upsilon_{2,0} & \cdots & \upsilon_{K,0} \\ \vdots & \vdots & \ddots & \vdots \\ \upsilon_{1,0} & \upsilon_{2,0} & \cdots & \upsilon_{K,0} \end{bmatrix}. \tag{25}$$

Then Equation (13) can be rewritten as

$$\mathbf{C}_B \approx \boldsymbol{\Upsilon}_0 \odot \mathbf{C}_A = \mathbf{C}_A \boldsymbol{\Psi}_0, \tag{26}$$

where $\boldsymbol{\Psi}_0$ is a diagonal matrix, defined by $\boldsymbol{\Psi}_0 = \mathrm{diag}(\upsilon_{1,0}, \upsilon_{2,0}, \ldots, \upsilon_{K,0})$.

Using Equation (26), Equation (16) can be rewritten as

$$\begin{bmatrix} \mathbf{C}_A \\ \mathbf{C}_B \end{bmatrix} \approx \begin{bmatrix} \mathbf{C}_A \\ \mathbf{C}_A \boldsymbol{\Psi}_0 \end{bmatrix} = \mathbf{U}_s \mathbf{F}_0 = \begin{bmatrix} \mathbf{U}_{s1} \\ \mathbf{U}_{s2} \end{bmatrix} \mathbf{F}_0, \tag{27}$$

where $\mathbf{F}_0$ is the approximate matrix of $\mathbf{F}$.

Therefore, it can be given by

$$\begin{aligned} \mathbf{U}_{s1} &\approx \mathbf{C}_A \mathbf{F}_0^{-1} \\ \mathbf{U}_{s2} &\approx \mathbf{C}_B \mathbf{F}_0^{-1} = \mathbf{C}_A \boldsymbol{\Psi}_0 \mathbf{F}_0^{-1} \end{aligned}. \tag{28}$$

Further, it can be written as

$$\mathbf{F}_0\mathbf{\Psi}_0\mathbf{F}_0^{-1} \approx (\mathbf{U}_{s1})^{\dagger}\mathbf{U}_{s2}. \tag{29}$$

By eigen-decomposition of $(\mathbf{U}_{s1})^{\dagger}\mathbf{U}_{s2}$, $\mathbf{\Psi}_0$ and $\mathbf{F}_0$ can be obtained. Then $\mathbf{\Upsilon}_0$ can be computed by Equation (25).

3.2.3. Iterative Estimation

With the obtained initial matrix $\mathbf{F}_0$, the iterative estimation method is described in Table 1.

Table 1. Operation of the iterative algorithm.

Initialization: Given N received snapshots $\mathbf{x}_A(t)$ and $\mathbf{x}_B(t)$, compute the covariance matrix $\mathbf{R} = E[\mathbf{x}(t)\mathbf{x}^H(t)]$, where $\mathbf{x}(t) = [\mathbf{x}_A(t), \mathbf{x}_B(t)]^T$. Compute the eigen-decomposition of $\mathbf{R}$ and obtain the estimation of the initial matrix $\mathbf{F_0}$.
Iteration: For $i = 1, 2, \ldots$ until the recursion is halted

(i) Based on Equation (19), the i-th estimation of matrix $\mathbf{\Upsilon}$ is

$$\mathbf{\Upsilon}(i) = (\mathbf{U}_{s2}\mathbf{F}(i-1))./(\mathbf{U}_{s1}\mathbf{F}(i-1)). \tag{30}$$

(ii) Normalize all elements of the matrix $\mathbf{\Upsilon}(i)$ and obtain

$$\upsilon_{m,k}(i) = \upsilon_{m,k}(i)/|\upsilon_{m,k}(i)|, \tag{31}$$

where $\upsilon_{m,k}(i)$ is the m-th row and k-th column element of matrix $\mathbf{\Upsilon}(i)$.

(iii) Based on Equation (19), compute

$$\mathbf{F}(i) = \mathbf{U}_{s2}^{\dagger}[(\mathbf{U}_{s1}\mathbf{F}(i-1)) \odot \mathbf{\Upsilon}(i)] \tag{32}$$

to update the matrix of $\mathbf{F}_i$.

(iv) Repeat steps (ii) and (iii), until the bias of $\mathbf{\Upsilon}(i)$ and $\mathbf{\Upsilon}(i-1)$ is less than the threshold ε,

$$\|\mathbf{\Upsilon}(i) - \mathbf{\Upsilon}(i-1)\|_F < \varepsilon \tag{33}$$

or iteration times are over the limit, the iteration ends.

Parameters Estimation: By exploiting the k-th column of $\mathbf{\Upsilon}$, angles $\theta_{k,m}(m = 1, 2, \ldots, M)$ that the k-th source impinging upon each doublets can be obtained, and to near-field sources, the corresponding distance r_k that the source impinging on the reference element can be successively obtained.

The k-th column of $\mathbf{\Upsilon}$ is $\boldsymbol{\upsilon}_k$, and it denotes the information of k-th source angles. With the definition in Equation (7), angles can be estimated by

$$\hat{\theta}_{k,m} = \arcsin\left(\frac{(\angle\upsilon_{k,m})\,\lambda}{2\pi d}\right), \tag{34}$$

where symbol $(\angle)$ denotes the phase angle of complex.

Using the estimated angles for the k-th source, the type of sources corresponding to the array can be determined. When the estimated angles of the k-th sources satisfy

$$\left|\hat{\theta}_{k,1} - \hat{\theta}_{k,M}\right| \leqslant \varepsilon_{NF}, \tag{35}$$

where ε_{NF} is the threshold. Note that if Equation (35) holds, the source is located at the far-field of array. Otherwise, the source is located at the near-field of array.

It is obvious that when $\{\hat{\theta}_{k,1}, \hat{\theta}_{k,2}, \ldots, \hat{\theta}_{k,M}\}$ for the k-th source are separated enough, the source can be recognized to locate at the near-field of the array. Thus, the range of the k-th source can be estimated based on triangulation. Consider that the k-th source is near-field source, the geometry

relationship between the range $r_{k,1}$ and angles $\{\theta_{k,1}, \theta_{k,2}, \ldots, \theta_{k,M}\}$ corresponding to the k-th source can be presented as

$$\mathbf{z}r_1 = \mathbf{b}. \tag{36}$$

where $\mathbf{z} \triangleq [\sec(\theta_{k,2}), \sec(\theta_{k,3}), \ldots, \sec(\theta_{k,M})]^T$, $\mathbf{b} \triangleq [b_1, b_2, \ldots, b_{M-1}]^T$, with $b_m = csc(\theta_{k,1} - \theta_{k,m+1}) \sum_{i=1}^{m} D_m$. Then the range r_1 can be estimated by

$$r_1 = \mathbf{z}^{\dagger}\mathbf{b}. \tag{37}$$

While estimated angles $\{\hat{\theta}_{k,1}, \hat{\theta}_{k,2}, \ldots, \hat{\theta}_{k,M}\}$ of the k-th source are close to each other and the angles meet $\left|\hat{\theta}_{k,1} - \hat{\theta}_{k,M}\right| \leqslant \varepsilon_\theta$, the source can be detected to locate at far-field of the array, and the range of source cannot be estimated properly by employing Equation (37).

4. ANALYSIS AND SIMULATION

4.1. Analysis for the Proposed Signal Model

In this section, the advantage of the proposed signal model is analysed.

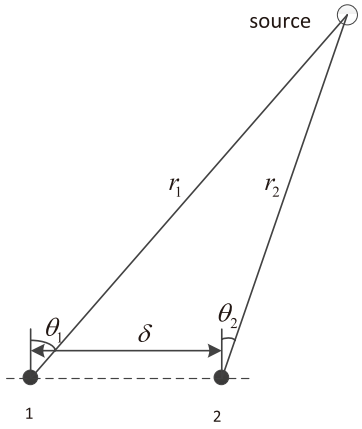

Figure 3. The geometry of two sensors array.

First, let us consider an array with two elements as shown in Fig. 3. The displacement between the two sensors is δ. Suppose that the first element is the common reference element. The phase shift associated with the propagation time delay between the first sensor and second sensor of the source signal is

$$\tau(\delta) = 2\pi(r_2 - r_1)/\lambda, \tag{38}$$

where r_1 is the range between the source and reference element. r_2 is given by

$$r_2 = \sqrt{r_1^2 + \delta^2 - 2r_1\delta\sin\theta_1}. \tag{39}$$

Utilizing Fresnel approximation, Equation (38) approximately equals

$$\hat{\tau}(\delta) \approx -\frac{2\pi}{\lambda}\sin\theta_1 + \frac{\pi\delta^2}{\lambda r_1}\cos^2\theta_1. \tag{40}$$

Therefore, the bias between the approximate phase shift $\hat{\tau}(\delta)$ and real phase shift $\tau(\delta)$ is

$$\begin{aligned}\Delta\tau(\delta) &= \tau(\delta) - \hat{\tau}(\delta) \\ &= \frac{2\pi r_1}{\lambda}\left[\left(\sqrt{1 + \left(\frac{\delta}{r_1}\right)^2 - 2\frac{\delta}{r_1}\sin\theta_1} - 1\right) - \left(-\frac{\delta}{r_1}\sin\theta_1 + 2\left(\frac{\delta}{r_1}\right)^2\cos^2\theta_1\right)\right].\end{aligned} \tag{41}$$

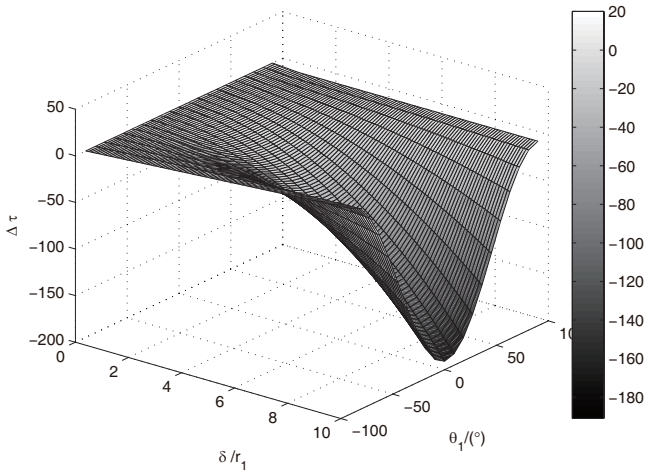

Figure 4. The bias of Fresnel approximate against θ_1 and δ/r_1.

The bias $\Delta\tau(\delta)$ varying with the direction of source θ_1 and δ/r_1 is shown in Fig. 4. Note that the item $2\pi r_1/\lambda$ is ignored in the simulation of Fig. 4. It is obvious that the bias $\Delta\tau(\delta)$ increases versus δ/r_1 when θ_1 is fixed. With δ/r_1 fixed, the bias also increases when θ_1 is close to 0°. It can also be seen that the smaller the displacement δ is, the smaller the bias $\Delta\tau(\delta)$ is. It denotes that the bias $\Delta\tau(\delta)$ can be diminished when the small displacement δ between two elements is exploited.

In the paper, it is assumed that sources are located at far-field of each doublet, thus the displacement d of elements of each doublet satisfies $r_1 > 2d^2/\lambda$.

Based on numerical results in Fig. 4, the bias of different reference elements satisfies

$$\Delta\tau(d) \ll \Delta\tau(D) \tag{42}$$

where $\Delta\tau(d)$ and $\Delta\tau(D)$ are the corresponding bias. It is obvious that the model can avoid the mismatch of traditional Fresnel approximate model [15].

4.2. Threshold for the Iterative Algorithm

The matrix $\boldsymbol{\Upsilon}(i) - \boldsymbol{\Upsilon}(i-1)$ denotes the bias of two iterations, thus $\|\boldsymbol{\Upsilon}(i) - \boldsymbol{\Upsilon}(i-1)\|_F^2$ is written as

$$\|\boldsymbol{\Upsilon}(i) - \boldsymbol{\Upsilon}(i-1)\|_F^2 = \sum_{m=1}^{M}\sum_{k=1}^{K} \left|\upsilon_{k,m}(i) - \upsilon_{k,m}(i-1)\right|^2 \tag{43}$$

where $\upsilon_{k,m}(i) = \exp[j\frac{2\pi d}{\lambda}\sin\theta_{k,m}(i)]$. $\|\boldsymbol{\Upsilon}(i) - \boldsymbol{\Upsilon}(i-1)\|_F^2$ is the sum of the bias of all elements.

When the error margin ε_θ of DOA estimation is fixed, the norm of bias matrix can be obtained. Suppose that when the error margin is $\varepsilon_\theta = |\theta_{k,m}(i) - \theta_{k,m}(i-1)| \geq 0$, iterations end. Then every element of matrix $\boldsymbol{\Upsilon}(i) - \boldsymbol{\Upsilon}(i-1)$ satisfies

$$\left|\upsilon_{k,m}(i) - \upsilon_{k,m}(i-1)\right|^2 \approx 2 - 2\cos\left\{2\pi d\varepsilon_\theta \cos\theta_{k.m}(i-1)/\lambda\right\} \tag{44}$$

where ε_θ is considered to be less than 0.1°.

Due to $\theta_{k,m}(i-1) \in \left[-\frac{\pi}{2}, \frac{\pi}{2}\right]$, $\cos\theta_{k.m}(i-1) \in [-1, 1]$. Thus, Equation (44) can be obtained

$$\left|\upsilon_{k,m}(i) - \upsilon_{k,m}(i-1)\right|^2 \leqslant 2 - 2\cos(2\pi d\varepsilon_\theta/\lambda) \tag{45}$$

The bias matrix is given by

$$\begin{aligned}\|\boldsymbol{\Upsilon}(i) - \boldsymbol{\Upsilon}(i-1)\|_F &\leqslant \sqrt{2MK\left[1 - \cos(2\pi d\varepsilon_\theta/\lambda)\right]} \\ &= 2\sqrt{MK}\sin\left(\pi d\varepsilon_\theta/\lambda\right).\end{aligned} \tag{46}$$

Therefore, the threshold ε of the iterative algorithm can be set as

$$\varepsilon = 2\sqrt{MK}\sin\left(\pi d\varepsilon_\theta/\lambda\right). \tag{47}$$

Based on the number of doublets and the number of sources, it is easy to obtain the iterative threshold.

4.3. Simulation

The first experiment is designed to illustrate iterative performance of the proposed algorithm. Two sources ($K = 2$) impinging on the independent doublets arrays are considered. The array is constructed by a linear array with 5 doublets. The sensor spacing of each doublet is $d = 0.5\lambda$, and the spacing between doublets is $D_m = 10\lambda$, with $m = 1, 2, \ldots, M-1$. λ is the wavelength of source. DOAs are $\{\theta_1, \theta_2\} = \{-12^\circ, 40^\circ\}$, and the corresponding range is $\{r_1, r_2\} = \{200\lambda, 400\lambda\}$. It is obvious that the source is located at the near-field of array and the far-field of each doublet. The performance of iterative algorithm is evaluated with noise and noiselessness scenarios. The signal-to-noise ratio (SNR) is set to 5 dB. The number of snapshot is 2000.

The trend of $\|\boldsymbol{\Upsilon}_i - \boldsymbol{\Upsilon}_{i-1}\|_F$ in Equation (33) against iteration times is shown in Fig. 5, and the error of estimated parameters against iteration times is shown in Fig. 6. It is clear that though $\|\boldsymbol{\Upsilon}_i - \boldsymbol{\Upsilon}_{i-1}\|_F$ decreases steadily with iteration times increases, the estimation of parameters reaches stables values when the iteration times is about 15. The corresponding $\|\boldsymbol{\Upsilon}_i - \boldsymbol{\Upsilon}_{i-1}\|_F$ is about 10^{-4}. The result denotes that a suitable threshold can guarantee stable estimation results, whereas an improper threshold may result in excessive meaningless calculation. The results in Fig. 6 also denote that the proposed method is unbiased in the noise-free case.

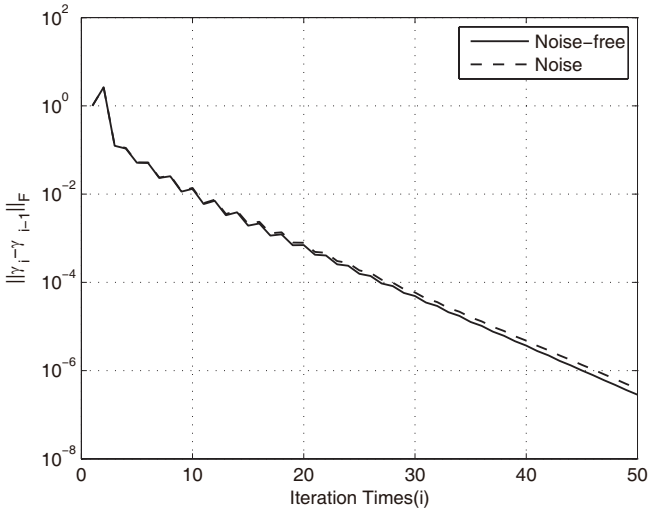

Figure 5. The trend of $\|\boldsymbol{\Upsilon}_i - \boldsymbol{\Upsilon}_{i-1}\|_F$ against iteration times.

In the second example, we evaluate the performance of the proposed algorithm with multiple sources. The root mean square of error (RMSE) of estimated angles is defined as

$$\mathrm{RMSE}\left(\theta_k\right) = \sqrt{\frac{1}{N}\sum_{n=1}^{N}\left(\theta_k - \hat{\theta}_k\left(n\right)\right)^2}, \tag{48}$$

where N is the number of Monte Carlo runs. The normalized root mean square of error (NRMSE) of estimated range is defined as

$$\mathrm{NRMSE}\left(r_k\right) = \sqrt{\frac{1}{N}\sum_{n=1}^{N}\left(\frac{r_k - \hat{r}_k\left(n\right)}{r_k}\right)^2}. \tag{49}$$

Three sources impinging upon the array are considered in this example. The DOAs of three sources are $\{\theta_1, \theta_2, \theta_3\} = \{-30^\circ, 40^\circ, 15^\circ\}$, and the range is $\{r_1, r_2, r_3\} = \{200\lambda, 400\lambda, 300\lambda\}$. The number of snapshots is 2000. The simulation results against SNR are reported in Fig. 7. It is displayed that the proposed algorithm can deal with multiple sources that impinge upon independent doublets arrays,

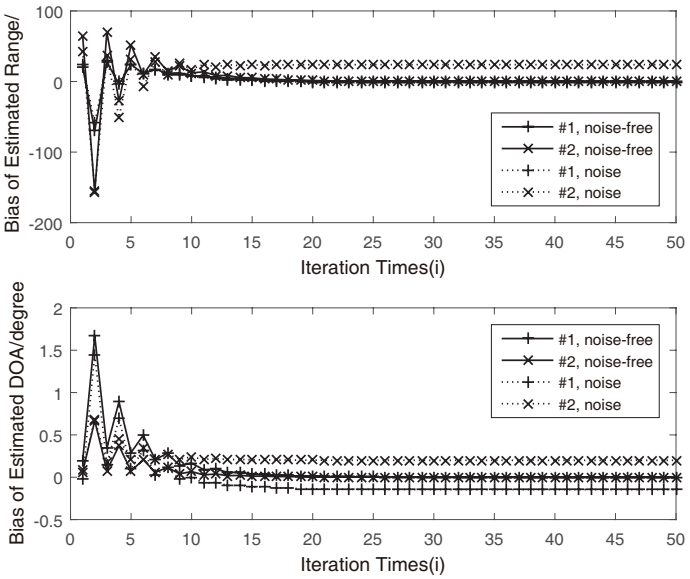

Figure 6. The error of DOA and range estimation against iteration times.

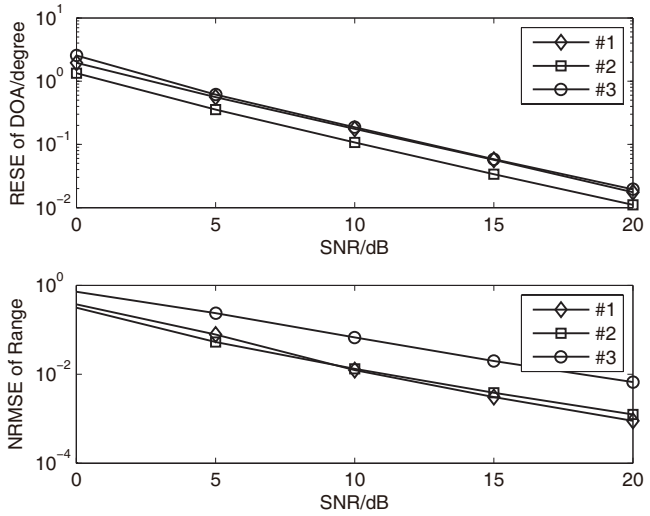

Figure 7. RMSEs of DOA estimation and NRMSEs of range estimation against SNR.

and the estimation performance of parameters increases with SNR increases. Note that the traditional algorithm can only deal with coherent array which employs a common oscillator, or different oscillators with complicated phase synchronization device. Comparing those algorithms, the proposed algorithm indicates that location problem only requires multiple doublets to decouple multiple sources. Therefore, it can reduce the difficulty of implementation.

The third simulation experiment illustrates the advantage of the proposed algorithm, compared with the cross location with multiple interferometers (CLMI). The CLMI method employs each doublet as an interferometer to obtain the DOA of source [34] and then obtains the location of source by triangulation as well as the proposed method. The CLMI can only deal with the location problem for single source, thus this simulation entails one source ($K = 1$), with (angle, range) equal to $\theta_1 = -12°$, $r_1 = 200\lambda$. The array is the same as the first experiments. The sample of snapshots snapshot is 2000.

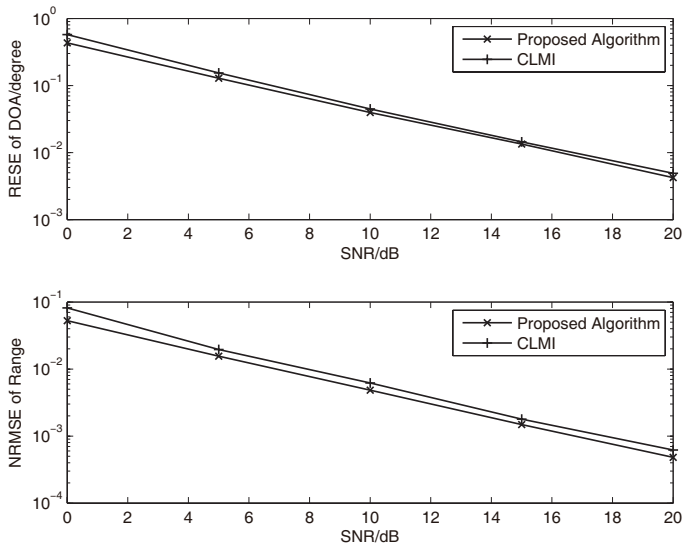

Figure 8. RMSEs of DOA estimation and NRMSEs of range estimation against SNR.

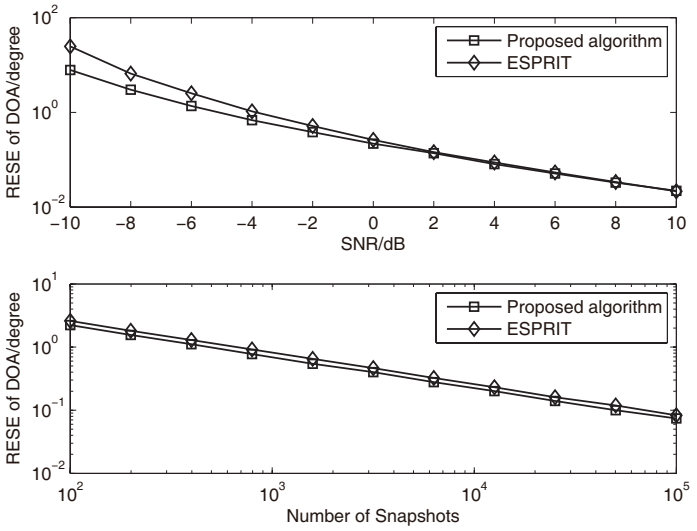

Figure 9. RMSEs of DOA estimation against SNR and Snapshots.

The performance of algorithms against SNR is obtained over 1000 independent trials.

The results are shown in Fig. 8 in terms of angle and range RMSE, respectively. It is shown that the performance of the proposed method and CLMI increases with SNR. When the SNR is higher than 4 dB, the estimation results of DOA and range are acceptable. The proposed method yields a better performance improvement than CLMI. The performance gap is due to the effective utilization of the doublets array.

In the fourth example, we compare the performance of the proposed algorithm with the ESPRIT algorithm [7]. The array utilized is the same as the former experiment. The incoming signal is a far-field source, with $\theta = -30°$. It is considered that the estimated DOA by ESPRIT is obtained with five doublets, respectively, and the corresponding performance is gained by all the estimated DOA results. The proposed algorithm uses all data received by the five doublets together, and the threshold of it is $\varepsilon = 10^{-5}$. The performance of estimated angle against SNR (with 10000 snapshots) and snapshots (with 0 dB SNR) is obtained by 500 independent trials and shown in Fig. 9.

The first result of Fig. 9 indicates that, for low SNR, the performance of the proposed algorithm is better than the ESPRIT algorithm. When the SNR is higher, the proposed algorithm achieves close performance to the ESPRIT. The second result suggests that the proposed algorithm has better DOA estimation performance than ESPRIT against different snapshots. It shows that the iterative algorithm performs better than ESPRIT, especially at lower SNR. Obviously, the proposed algorithm can gain better performance for its effective exploitation of the array.

In the last simulation example, the scenario of mixed sources is considered. The scenario includes one far-field source located at $\theta_1 = -30°, r_1 = 2 \times 10^6\lambda$ and one near-field source located at $\theta_2 = 45°, r_2 = 400\lambda$, respectively. The threshold of iterative algorithm is set as $\varepsilon = 10^{-4}$. The SNR varies from 0 dB to 20 dB. Fig. 10 provides the simulation result. It is observed that the proposed method can deal with the scenario of mixed sources, and the conclusion that other algorithms cannot handle far-field source in the previous analysis is verified.

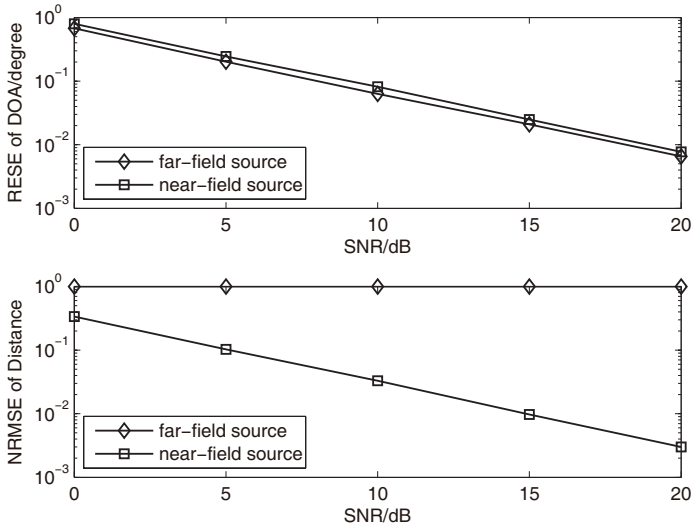

Figure 10. RMSEs of DOA estimation and NRMSEs of range estimation against SNR.

5. CONCLUSION

In this paper, we have presented an iterative algorithm for the location of multiple sources based on independent doublets arrays. Based on the array, the proposed algorithm introduces a unified signal model for near-field sources or(and) far-field sources. Especially for near-field sources, the signal model could passably avoid the bias of Fresnel approximate because of the close displacement between elements of each doublet. Since only the rotational invariance relationship towards each doublet was employed, the proposed algorithm could avoid complicated phase synchronization among doublets. Further, the spacing between two adjacent doublets can be set larger to achieve greater array aperture for good resolution. The proposed algorithm utilized the whole received data efficiently and could handle more than two sources with only two sensors in each doublet. This algorithm also provides a simple calculation method to reach acceptable estimation results. For far-field sources, the proposed algorithm achieved better performance than ESPRIT. For near-field sources, the algorithm performs better than CLMI. To sum up, the present algorithm based on independent doublets array has many benefits and reduces the difficulty of implementation.

APPENDIX A. THE MAXIMUM LIKELIHOOD ESTIMATOR

In this section, the Maximum Likelihood (ML) estimator of parameters estimation is derived for source location.

Under the assumptions of the observation process $\mathbf{X}(t_n)$, constitute a stationary zero mean Gaussian random process, and its second-order moments are

$$\begin{aligned}\mathbf{R}x &= E\left[\mathbf{X}\left(t_1\right)\mathbf{X}^H(t_2)\right] \\ &= \left[\begin{pmatrix}\mathbf{C}_A \\ \mathbf{C}_B\end{pmatrix}\mathbf{R}_s\begin{pmatrix}\mathbf{C}_A \\ \mathbf{C}_B\end{pmatrix}^H + \sigma^2\mathbf{I}\right]\delta_{t1,t2},\end{aligned} \tag{A1}$$

where $\delta_{t1,t2}$ represents the Kronecker delta.

The likelihood function of N snapshots $\mathbf{X}(t_1)$, $\mathbf{X}(t_2)$, ...,$\mathbf{X}(t_N)$ is

$$p\left(\mathbf{X}\left(t_1\right),\mathbf{X}\left(t_2\right),\ldots,\mathbf{X}\left(t_N\right)\middle|\,\theta,\mathbf{r},\mathbf{R}_s,\sigma^2,\mathbf{\Phi}\right) = \prod_{n=1}^{N}\frac{1}{\pi^M\det\left(\mathbf{R}\right)}e^{-\mathbf{X}^H(t_i)\mathbf{R}^{-1}\mathbf{X}(t_i)}, \tag{A2}$$

The negative log-likelihood function is

$$-\log\left[p\left(\boldsymbol{\theta},\mathbf{r},\mathbf{R}_s,\sigma^2,\mathbf{\Phi}\right)\right] = MN\log\pi + N\log\det\left(\mathbf{R}\right) + \sum_{i=1}^{N}\mathbf{X}^H\left(t_i\right)\mathbf{R}^{-1}\mathbf{X}\left(t_i\right). \tag{A3}$$

Ignoring the constant term and normalizing by the number of snapshot N, the parameters estimation is obtained by solving the optimization problem as follows,

$$\left\{\hat{\boldsymbol{\theta}},\hat{\mathbf{r}},\hat{\mathbf{R}}_s,\hat{\sigma}^2,\hat{\mathbf{\Phi}}\right\} = \arg\min_{\boldsymbol{\theta},\mathbf{r},\mathbf{R}_s,\sigma^2,\mathbf{\Phi}} l\left(\boldsymbol{\theta},\mathbf{r},\mathbf{R}_s,\sigma^2,\mathbf{\Phi}\right), \tag{A4}$$

where

$$l\left(\boldsymbol{\theta},\mathbf{r},\mathbf{R}_s,\sigma^2,\mathbf{\Phi}\right) = \log\det\left(\mathbf{R}\right) + \frac{1}{N}\sum_{i=1}^{N}\mathbf{X}^H\left(t_i\right)\mathbf{R}^{-1}\mathbf{X}\left(t_i\right) = \log\det\left(\mathbf{R}\right) + Tr\left\{\mathbf{R}^{-1}\hat{\mathbf{R}}\right\}, \tag{A5}$$

is the criterion function and

$$\hat{\mathbf{R}} = \frac{1}{N}\sum_{i=1}^{N}\mathbf{X}^H\left(t_i\right)\mathbf{X}\left(t_i\right), \tag{A6}$$

is the sample covariance matrix.

The estimates of the signal sources covariance matrix and the noise variance are [35, 36]

$$\hat{\mathbf{R}}_s\left(\boldsymbol{\theta},\mathbf{r},\mathbf{\Phi}\right) = \begin{bmatrix}\mathbf{C}_A \\ \mathbf{C}_B\end{bmatrix}^{\dagger}\left(\hat{\mathbf{R}} - \hat{\sigma}^2\left(\boldsymbol{\theta},\mathbf{r},\mathbf{\Phi}\right)\right)\left\{\begin{bmatrix}\mathbf{C}_A \\ \mathbf{C}_B\end{bmatrix}^{\dagger}\right\}^H \tag{A7}$$

$$\hat{\sigma}^2\left(\boldsymbol{\theta},\mathbf{r},\mathbf{\Phi}\right) = \frac{1}{M-K}Tr\left\{\mathbf{P}_{A,B}^{\perp}\hat{\mathbf{R}}\right\}, \tag{A8}$$

where the superscript $(\cdot)^{\dagger}$ denotes Moore-Penrose inverse. $\mathbf{P}_{A,B}^{\perp}$ is the orthogonal projector onto the null space of $\begin{bmatrix}\mathbf{C}_A \\ \mathbf{C}_B\end{bmatrix}^H$,

$$\mathbf{P}_{A,B}^{\perp} = \mathbf{I} - \begin{bmatrix}\mathbf{C}_A \\ \mathbf{C}_B\end{bmatrix}\begin{bmatrix}\mathbf{C}_A \\ \mathbf{C}_B\end{bmatrix}^{\dagger}. \tag{A9}$$

Substitute Equation (A7) and Equation (A8) into Equation (A5), then the parameters estimates are obtained by solving the following optimization problem

$$\{\boldsymbol{\theta},\mathbf{r},\mathbf{\Phi}\} = \arg\min_{\boldsymbol{\theta},\mathbf{r},\mathbf{\Phi}}\log\det\mathbf{G}, \tag{A10}$$

where $\mathbf{G} = \begin{bmatrix}\mathbf{C}_A \\ \mathbf{C}_B\end{bmatrix}\hat{\mathbf{R}}_s(\boldsymbol{\theta},\mathbf{r},\mathbf{\Phi})\begin{bmatrix}\mathbf{C}_A \\ \mathbf{C}_B\end{bmatrix}^H + \hat{\sigma}^2(\boldsymbol{\theta},\mathbf{r},\mathbf{\Phi})\mathbf{I}$.

It is obvious that the ML algorithm is a multivariate nonlinear maximization and can be solved with quite high computational load.

REFERENCES

1. Rajagopal, R. and P. R. Rao, "Generalised algorithm for DOA estimation in a passive sonar," *Radar and Signal Processing, IEE Proceedings F*, Vol. 140, 12–20, 1993.
2. Macphie, R. H., "Thinned coincident arrays for the direct measurement of the principal solution in radio astronomy," *IEEE Transactions on Antennas and Propagation*, Vol. 51, 788–793, 2003.
3. Arslan, G. and F. A. Sakarya, "A unified neural-network-based speaker localization technique," *IEEE Transactions on Neural Networks*, Vol. 11, 997–1002, 2000.
4. Tichavsky, P., K. T. Wong, and M. D. Zoltowski, "Near-field/far-field azimuth and elevation angle estimation using a single vector hydrophone," *IEEE Trans. Signal Process.*, Vol. 49, 2498–2510, 2001.
5. Krim, H. and M. Viberg, "Two decades of array signal processing research: The parametric approach," *IEEE Signal Processing Magazine*, Vol. 13, 67–94, 1996.
6. Schmidt, R. O., "Multiple emitter location and signal parameter estimation," *IEEE Transactions on Antennas and Propagation*, Vol. 34, 276–280, 1986.
7. Roy, R. and T. Kailath, "ESPRIT-estimation of signal parameters via rotational invariance techniques," *IEEE Transactions on Acoustics, Speech and Signal Processing*, Vol. 37, 984–995, 1989.
8. Yung-Dar, H. and M. Barkat, "Near-field multiple source localization by passive sensor array," *IEEE Transactions on Antennas and Propagation*, Vol. 39, 968–975, 1991.
9. Lee, J. H., D. H. Park, G. T. Park, and K. K. Lee, "Algebraic path-following algorithm for localising 3-D near-field sources in uniform circular array," *Electronics Letters*, Vol. 39, 1283–1285, 2003.
10. Wanjun, Z. and M. Y. W. Chia, "Near-field source localization via symmetric subarrays," *IEEE Signal Processing Letters*, Vol. 14, 409–412, 2007.
11. Junli, L. and L. Ding, "Passive localization of near-field sources using cumulant," *IEEE Sensors Journal*, Vol. 9, 953–960, 2009.
12. Chen, J. C., R. E. Hudson, and K. Yao, "Maximum-likelihood source localization and unknown sensor location estimation for wideband signals in the near-field," *IEEE Trans. Signal Process.*, Vol. 50, No. 8, 1843–1854, Aug. 2002.
13. Kabaoğlu, N., H. A. Çırpan, E. Çekli, and S. Paker, "Deterministic maximum likelihood approach for 3-d near field source localization," *AEU — International Journal of Electronics and Communications*, Vol. 57, 345–350, 2003.
14. Grosicki, E., K. Abed-Meraim, and Y. Hua, "A weighted linear prediction method for near-field source localization," *IEEE Trans. Signal Process.*, Vol. 53, 3651–3660, 2005.
15. Swindlehurst, A. L. and T. Kailath, "Passive direction-of-arrival and range estimation for near-field sources," *Fourth Annual ASSP Workshop on in Spectrum Estimation and Modeling, 1988*, 123–128, 1988.
16. Yu-Sheng, H., K. T. Wong, and L. Yeh, "Mismatch of near-field bearing-range spatial geometry in source-localization by a uniform linear array," *IEEE Transactions on Antennas and Propagation*, Vol. 59, 3658–3667, 2011.
17. Stansfield, R. G., "Statistical theory of d.f. fixing," *Electrical Engineers — Part IIIA: Radiocommunication, Journal of the Institution of*, Vol. 94, 762–770, 1947.
18. M. Gavish and A. J. Weiss, "Performance analysis of bearing-only target location algorithms," *IEEE Transactions on Aerospace and Electronic Systems*, Vol. 28, 817–828, 1992.
19. L. M. Kaplan, L. Qiang, and N. Molnar, "Maximum likelihood methods for bearings-only target localization," *2001 IEEE International Conference on Acoustics, Speech, and Signal Processing, 2001. Proceedings. (ICASSP'01)*, Vol. 5, 3001–3004, 2001.
20. Taff, L. G., "Target localization from bearings-only observations," *IEEE Transactions on Aerospace and Electronic Systems*, Vol. 33, 2–10, 1997.

21. Athley, F. and C. Engdahl, "Direction-of-arrival estimation using separated subarrays," *Conference Record of the Thirty-Fourth Asilomar Conference on Signals, Systems and Computers, 2000*, Vol. 1, 585–589, 2000.
22. Engdahl, C. and P. Sunnergren, "Model-based adaptive detection and DOA estimation using separated sub-arrays," *Proceedings of the IEEE in Radar Conference, 2002*, 104–109, 2002.
23. Vorobyov, S. A., A. B. Gershman, and W. Kon Max, "Maximum likelihood direction-of-arrival estimation in unknown noise fields using sparse sensor arrays," *IEEE Trans. Signal Process.*, Vol. 53, 34–43, 2005.
24. Jiang, J. C., P. Wei, and L. Gan, "Source location based on independent doublet array," *Electronics Letters*, Vol. 49, 907–908, 2013.
25. Hua, Q. D., T. N. Osterdock, and D. C. Westcott, "GPS synchronized frequency/time source," Google Patents, 1995.
26. Frey, R. L. and B. W. I. Kenneth, "Very low power high accuracy time and frequency circuits in GPS based tracking units," Google Patents, 1999.
27. Wang, W.-Q., "GPS-based time & phase synchronization processing for distributed SAR," *IEEE Transactions on Aerospace and Electronic Systems*, Vol. 45, 1040–1051, 2009.
28. Cheng, C.-L., F.-R. Chang, and K.-Y. Tu, "Highly accurate real-time GPS carrier phase-disciplined oscillator," *IEEE Transactions on Instrumentation and Measurement*, Vol. 54, 819–824, 2005.
29. Allan, D. W., N. Ashby, and C. C. Hodge, *The Science of Timekeeping*, Hewlett-Packard, 1997.
30. Lombardi, M. A., "The use of GPS disciplined oscillators as primary frequency standards for calibration and metrology laboratories," *Measure: The Journal of Measurement Science*, Vol. 3, 56–65, 2008.
31. Krieger, G. and M. Younis, "Impact of oscillator noise in bistatic and multistatic SAR," *Geoscience and Remote Sensing Letters, IEEE*, Vol. 3, 424–428, 2006.
32. Wang, W. Q., C. B. Ding, and X. D. Liang, "Time and phase synchronisation via direct-path signal for bistatic synthetic aperture radar systems," *Radar, Sonar & Navigation, IET*, Vol. 2, 1–11, 2008.
33. Styan, G. P. H., "Hadamard products and multivariate statistical analysis," *Linear Algebra and Its Applications*, Vol. 6, 217–240, 1973.
34. Ying-Wah, W., S. Rhodes, and E. H. Satorius, "Direction of arrival estimation via extended phase interferometry," *IEEE Transactions on Aerospace and Electronic Systems*, Vol. 31, 375–381, 1995.
35. Böhme, J. F., "Estimation of spectral parameters of correlated signals in wavefields," *Signal Processing*, Vol. 11, 329–337, 1986.
36. Ottersten, B., M. Viberg, P. Stoica, and A. Nehorai, "Exact and Large Sample Maximum Likelihood Techniques for Parameter Estimation and Detection in Array Processing," *Radar Array Processing*, Vol. 25, 99–151, S. Haykin, J. Litva, and T. Shepherd (eds.), Springer, Berlin Heidelberg, 1993.